frontiers | Frontiers in Materials

TYPE Original Research
PUBLISHED 28 October 2022
DOI 10.3389/fmats.2022.1054662

OPEN ACCESS

EDITED BY
Yu-Fei Wu,
RMIT University, Australia

REVIEWED BY
Ray Su,
The University of Hong Kong, Hong Kong SAR, China
Shan Gao,
Harbin Institute of Technology, China

*CORRESPONDENCE
Depeng Chen,
dpchen@ahut.edu.cn
Chunlin Liu,
chunlinliu@163.com

SPECIALTY SECTION
This article was submitted to Structural Materials, a section of the journal Frontiers in Materials

RECEIVED 27 September 2022
ACCEPTED 13 October 2022
PUBLISHED 28 October 2022

CITATION
Luo Y, Zhu Q, Chen D, Liu C and Pan S (2022), Steel rebar corrosion and corrosion-induced cracking in reinforced foamed concrete. *Front. Mater.* 9:1054662. doi: 10.3389/fmats.2022.1054662

Steel rebar corrosion and corrosion-induced cracking in reinforced foamed concrete

Yongheng Luo[1], Qilin Zhu[2], Depeng Chen[1]*, Chunlin Liu[1]* and Suiwei Pan[3]

[1]School of Architectural and Civil Engineering, Anhui University of Technology, Ma'anshan, China, [2]Shanghai Jianke Engineering Consulting Co. Ltd, Shanghai, China, [3]School of Construction Engineering, Maanshan University, Ma'anshan, China

This study investigated the corrosion behavior of steel rebar in foamed concrete and the effects of water-cement ratio, fly ash, and fiber on reinforced foamed concrete's corrosion rate and crack width. It was found that the corrosion rate of steel rebar and crack width of foamed concrete increased slowly with time and then developed rapidly, finally growing slowly. The higher the density of foamed concrete, the stronger the corrosion resistance of steel rebar. The best corrosion resistance of steel rebar in foamed concrete is achieved when the water-cement ratio is 0.5, fly ash and fiber are 20% and 0.6%, respectively.

KEYWORDS

foamed concrete, steel rebar corrosion rate, energize accelerated corrosion, density grade, crack width

1 Introduction

Compared with ordinary concrete, foamed concrete can significantly reduce self-weight, thus increasing the building height and reducing the project cost. Meanwhile, foamed concrete has excellent thermal performance and can be widely used in various thermal insulation structures. Assembled foamed concrete structures have a broad application prospect with good thermal insulation and high compressive strength. The assembled wall structures with foamed concrete are becoming the primary trend in the development of building envelope structures nowadays (Ganiron, 2016; Gu, 2018; Xiong and Shen, 2019). The immediate problem faced by reinforced foamed concrete structures is steel rebar corrosion, especially in buildings in coastal areas. The seaside or around-island environment is rich in chloride ions, and buildings in this environment are constantly subjected to salt spray and tide, which carry massive chloride ions. In the dry-wet cycle and periodic temperature changing, the corrosion process of steel rebar will be significantly accelerated, seriously affecting the average service life of buildings. Steel rebar in foamed concrete is easily corroded by chloride ions, especially when the thickness of the protective layer is inadequate. Cracking will appear in concrete slabs with large deflection and expansion stress generated by steel rebar corrosion. Therefore, the research on steel rebar corrosion in foamed concrete materials has important theoretical significance and practical value for revealing the evolution of steel rebar corrosion, improving the durability of reinforced foamed concrete materials, and promoting the application of reinforced foamed concrete.

Currently, most of the research on foamed concrete is focused on thermal performance and strength enhancement. There are only a few studies regarding the corrosion resistance of steel rebar and durability (Jones and Mccarthy, 2005; Lee et al., 2011; Remennikov et al., 2011; Roslan et al., 2012; Namsone et al., 2017). Roslan et al. (2012) found that adding fly ash to low-density foamed concrete improved the internal voids of concrete and reduced shrinkage. Jones and Mccarthy (2005) found that fly ash can improve the corrosion resistance of steel rebar in foamed concrete. Remennikov et al. (2011) explored the effect of fly ash content on the performance of foamed concrete. The results showed that when the fly ash content is too high, it will reduce the foamed concrete's strength. Existing studies (Huet et al., 2006; Surendranath and Harman, 2006; Marsavina et al., 2007; Shi and Xu, 2007) have shown that the electrochemical process of chloride ion corrosion on steel rebar has a complex rusting mechanism. Surendranath and Harman (2006) found that chloride ions acted mainly as depassivating agents in the corrosion process of steel rebar. The steel rebar started to rust after a potential difference was formed on the surface of the steel substrate. Marsavina et al. (2007), using fracture width as a variable, found that the greater the fracture width, the deeper the depth of chloride ion penetration.

By analyzing the test results of steel rebar corrosion rate and crack width, the development pattern of steel rebar corrosion in foamed concrete and the effects of water-binder ratio, fly ash, and fiber content on steel rebar corrosion rate and crack width in foamed concrete are studied. Meanwhile, the chloride ion diffusion behavior in foamed concrete is examined, and the relationship between steel rebar corrosion behavior and chloride ion diffusion behavior is established to reveal the mechanism of steel rebar corrosion in foamed concrete.

2 Experimental

2.1 Materials

Ordinary Portland cement of grade 42.5 was used as the binder in the concrete mixtures. The coarse aggregate was limestone gravel with a particle size range of 5–20 mm. The fine aggregate was natural river sand with a fineness modulus of 2.65. Grade II fly ash and polypropylene fiber of 9 mm length were adopted as concrete admixtures. HPB300 steel rebar with a nominal diameter of 6 mm was used.

2.2 Mix proportions

The mix proportions (Zhang et al., 2018; Liu et al., 2020) of C30 ordinary concrete and foamed concrete adopted are shown in Tables 1, 2.

TABLE 1 Mix proportions of C30 ordinary concrete (kg/m^3).

Cement	Sand	Gravel	Water
366	683	1160	194

2.3 Methods

2.3.1 Specimens preparation

The specimen size of foamed concrete and ordinary concrete, 100 × 100 × 100mm^3, were used for the steel rebar corrosion study. During the forming process, the steel rebar with a length of 120 mm was vertically inserted as the anode of the corrosion reaction system, making the thickness of the protective layer 35 mm and the exposed length of steel rebar 30 mm (smear epoxy resin for protection).

2.3.2 Accelerated corrosion method

The energized accelerated corrosion method was used to accelerate the corrosion process of steel rebar in foamed concrete, and the technique of controlling constant current was adopted for the test. The accelerating power supply used for this test is the model MT-152D DC regulated power supply with a maximum voltage of 15V, a maximum current of 2A, and a measurement accuracy of 0.001A.

Melchers and Sabine (Li and Melchers, 2005; Sabine and Raharinaivo, 2007) concluded that when the corrosion is accelerated by electrification, the corrosion products when the applied current density is below 200 $\mu A/cm^2$ are very close to the corrosion products in the natural environment. Maaddawy and Tang (Maaddawy and Soudki, 2007; Tang et al., 2014) both considered that the current density used in galvanic accelerated corrosion should not exceed 300 $\mu A/cm^2$. Under natural corrosion conditions, the corrosion current density is minimal, usually 0.1–100 $\mu A/cm^2$. Considering the corrosion pattern of steel rebar in the natural environment, the current density was set to 270 $\mu A/cm^2$. It is calculated that a current of 5 mA is required to achieve this current density setting. The foamed concrete specimens were immersed in NaCl solution, with the concentration of the solution always maintained at 3.5%. Make the solution 5 mm from the upper surface of the specimens, and a direct current was passed to accelerate the corrosion, as shown in Figure 1.

2.3.3 Measurement of corrosion rate

The specific measurement steps are as follows. 1) Breaking the corroded specimen into shape with a pressure tester, the residual mortar on the corroded steel rebar was eliminated by a steel brush. 2) Acid-washed and washed the corroded steel rebar, then immersed it in aqueous lime for neutralization. 3) The corroded steel rebar was dried in the oven (temperature was set at

TABLE 2 Mix proportions of foamed concrete with density as variable.

Density grade	Cement (kg)	Foam (L)	Water (kg)	Actual dry density (kg/m^3)
A04	333.33	0.944	166.67	423 ± 5
A05	416.67	0.854	208.34	491 ± 7
A06	500	0.765	250	615 ± 4
A07	583.33	0.677	291.67	704 ± 5
A08	666.67	0.587	333.34	812 ± 2
A09	750	0.498	375	897 ± 4
A10	833.33	0.409	416.67	996 ± 3

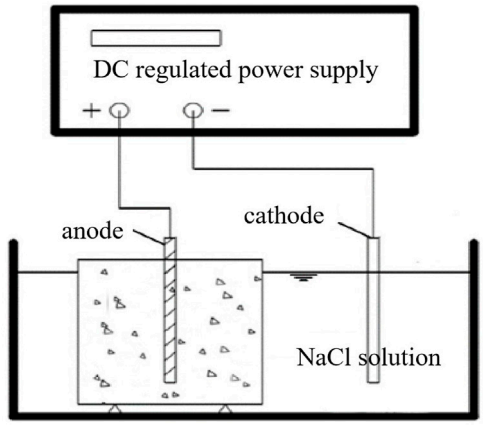

FIGURE 1
Schematic diagram of accelerated corrosion by electrification.

200 °C) for 4 hours, then weighed, and the corrosion rate was calculated according to Eq. 1.

$$\eta(\%) = \frac{m - m_1}{m} \times 100\% \quad (1)$$

In Eq. 1: η is the corrosion rate of the steel rebar; m is the initial weight of the steel rebar before it is inserted into the concrete specimen in g; m_1 is the weight of the corroded steel rebar after drying, in g.

2.3.4 Measurement of concrete crack width

The Crack Detector was used to measure the crack width of concrete. The detector adopts a new generation of arm high-speed processing platform, which can automatically read the crack width of concrete structures, bridges, subways, and other surfaces of different materials. It also features automatic data storage and image transfer. The maximum measurement width is 8mm, and the measurement accuracy is 0.01 mm.

2.3.5 Measurement method of chloride ion diffusion concentration

The foamed concrete specimens under different immersion times were drilled for powder in layers; the diameter of the drilled hole was 10 mm. The distance from the bottom of the borehole to the surface of the test piece was 0 ~ 5 mm, 5–10 mm, 10–15 mm, 15–20 mm, 20–25 mm, 25–30 mm, and 30–35 mm, respectively. Only the side with a protective layer thickness of 35 mm is retained as the chloride attack surface. The rest of the surface is sealed by epoxy resin. Each erosion surface drilled nine holes, with a hole spacing of 20 mm, and every three holes have taken powder for a group. The average value obtained after three measurements for each group of samples was used as the test result, while the results with more significant deviations were excluded.

The CLU-A portable rapid chloride content tester is used for chloride content measurement. The diffusion concentration of chloride ions was determined as follows. 1) Each layer of foamed concrete specimens with different soaking times was drilled to extract 30 g powders and ground, sieved the powder, and put in an oven for 2 hours. 2) Weigh 20 g of cooled powder into a triangular flask, add 120 ml deionized water to avoid hydrogen ions from disturbing the test results, and slowly pour the solution into a plastic cup after it is completely cloudy and left to stand. 3) After the solution standing for 24 h was filtered with filter paper, 30 ml of the solution was absorbed into a beaker to measure chloride ion content.

3 Results and discussion

3.1 Analysis of steel rebar corrosion

3.1.1 Effect of acceleration time on corrosion of steel rebar

According to energized acceleration test, corrosion specimens can be quickly obtained for studying the corrosion behavior of steel rebar (Ahmad, 2003; Maaddawy and Soudki, 2003; Vu and Stewart, 2005; Ha et al., 2007; Al-Harthy et al., 2011). Al-Harthy et al. (2011) concluded that the

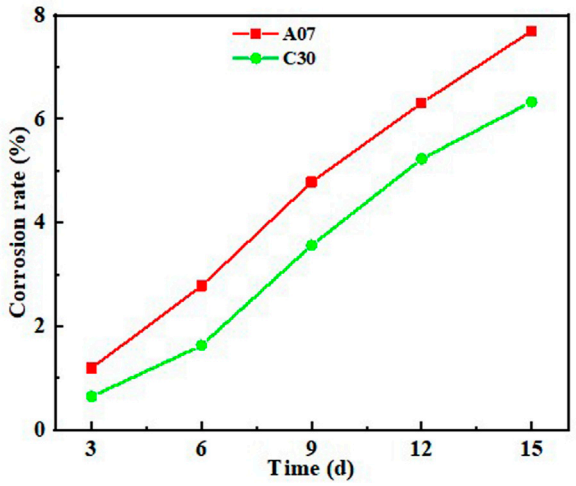

FIGURE 2
Corrosion rate with time.

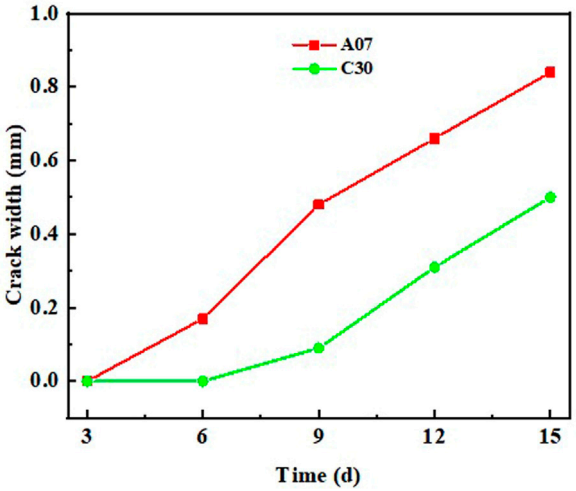

FIGURE 3
Crack width with time.

steel rebar would show uniform corrosion after energized acceleration test. Vu and Stewart (2005) used the energized accelerated corrosion method to establish a crack extension model. Ahmad (2003) similarly adopted the energized accelerated corrosion method to obtain an empirical formula for the corrosion depth of steel rebar when concrete is cracked.

Foamed concrete is often used as insulation material below the A04 level. It can be both load-bearing and insulation between A05 and A07 levels. When it is above grade A08, it is often used for load-bearing structures. Therefore, to

TABLE 3 Function fitting value and fitting correlation degree.

	Nonlinear curve fitting value	R^2
Corrosion rate	$y = -0.8312e^{\frac{x}{9.73}} + 6.2342$	0.9828
Crack width	$y = -1.2241e^{\frac{x}{29.10}} + 2.0435$	0.9868

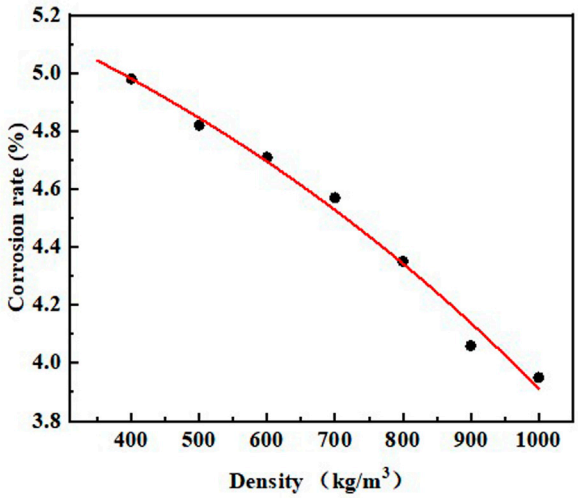

FIGURE 4
Corrosion rate with density grade.

ensure the thermal performance and strength of the wallboard, the A07 grade foamed concrete was selected for the test. The power supply was turned off for ordinary concrete specimens, and A07 foamed concrete specimens after accelerated corrosion for 3, 6, 9, 12, and 15 days. Each group of specimens includes three specimens, and the average value of the three test specimens was taken as the test result of this group. The steel rebar corrosion rate and crack width measurements are shown in Figures 2, 3.

As seen in Figure 2, the steel rebar corrosion rate of both ordinary concrete specimens and foamed concrete specimens increases slowly at the initial stage of energized acceleration. The corrosion rate of steel rebar showed a trend of slow increase, then rapid development, and finally, slow increase with time. The main reasons are as follows. At the initial stage of corrosion, only a tiny part of the oxygen and moisture that caused corrosion can reach the steel rebar through the protective layer, so the corrosion rate is slow. As time increases, the amount of oxygen and chloride ions required for the corrosion is gradually sufficient, and the steel rebar enters the stage of rapid corrosion. In the later stage of corrosion, increased corrosion products cannot penetrate cracks in time and cover the steel rebar surface, and the

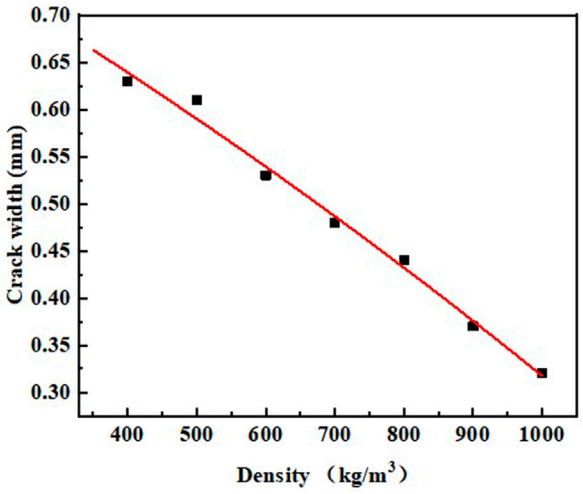

FIGURE 5
Crack width with density grade.

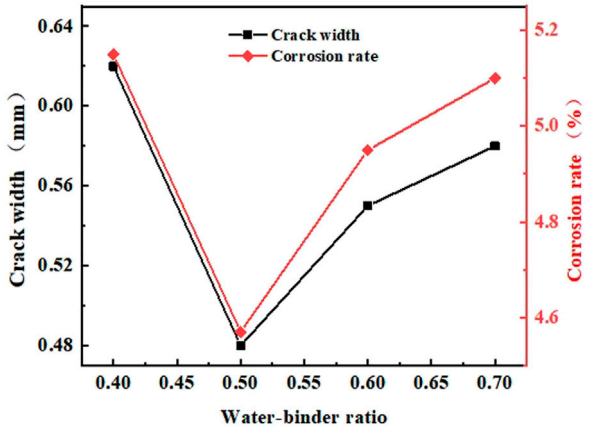

FIGURE 6
Corrosion rate and crack width with water-binder ratio.

anodic reaction is prevented. The corrosion products also block the pores in the mortar around the steel rebar, making it difficult for oxygen and water to enter. Therefore the corrosion rate of the steel rebar is gradually slowed down again.

As seen in Figure 3, foamed concrete cracks earlier than ordinary concrete. After 15 days of energized acceleration test, the crack width of foamed concrete was 1.68 times that of ordinary concrete. Ordinary concrete's strength and internal density are stronger than foamed concrete, so it is difficult for a small number of corrosion products to cause ordinary concrete cracking.

3.1.2 Effect of density grade on corrosion of steel rebar

The density grade of foamed concrete significantly affects compressive strength, water absorption, and drying shrinkage (Amran et al., 2015; Hilal et al., 2015; Falliano et al., 2019). However, there are fewer studies on the relationship between the corrosion resistance of steel rebar and the density grade of foamed concrete. The change in corrosion behavior of the steel rebar was most apparent at 9 days of continuously energized corrosion, so specimens with 9 days of continuously energized corrosion were selected for subsequent tests. Three test specimens were used for each density grade, and the average value of the results of the three test specimens was taken as the final test result.

As seen in Figure 4, the higher the density grade of foamed concrete, the lower the corrosion rate of steel rebar. The severity of steel rebar corrosion after 9 days of continuously energized corrosion is A04 > A05 > A06 > A07 > A08 > A09 > A10. For the same rusting time, the highest corrosion rate of 4.98% was found in the foamed concrete specimen with density grade A04, 4.57% in the steel rebar when the density grade was increased to A07, and the lowest corrosion rate of 3.95% in the foamed concrete with grade A10. As seen in Figure 5, the crack width on the foamed concrete surface decreases gradually with the increase of the density grade, and the crack appearance time is delayed continuously. There is an exponential relationship between the density grade of foamed concrete and the steel rebar corrosion rate and crack width. The fair value of the nonlinear function and the fitting correlation coefficient are shown in Table 3.

To sum up, it can be concluded that the higher the density grade of foamed concrete, the stronger the corrosion resistance of steel rebar. The main reason is that with the increase of the density grade of foamed concrete, the internal connecting holes and big holes are reduced. This increases the contact surface between the gelled material and the adhesive, eventually increasing foamed concrete compactness and reducing internal defects. The resistance of the foamed concrete specimen to cracking increases, the crack width decreases, and the corrosion resistance is enhanced.

3.2 Effect of internal factors on corrosion of steel rebar

The specimens were prepared following the mix proportions for A07 grade foamed concrete. Three specimens were used for each group of tests, and the average of the results of the three specimens was taken as the final test results.

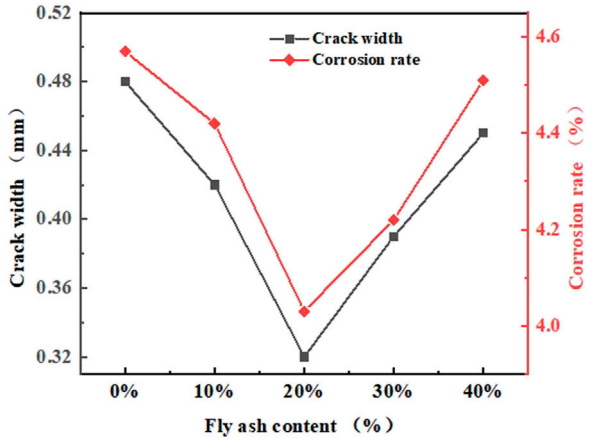

FIGURE 7
Corrosion rate and crack width with fly ash content.

3.2.1 Effect of water-binder ratio on corrosion resistance of steel rebar

The trends of the corrosion rate of steel rebar and the corrosion-induced cracking width with the water-cement ratio can be seen in Figure 6.

It is clear that with the increase of the water-binder ratio, the corrosion of steel rebar decreases first and then increases. That is, the corrosion resistance of steel rebar strengthens first and then weakens. When the water-binder ratio is 0.5, the corrosion rate of steel rebar is the lowest, only 4.57%. The crack width of foamed concrete showed the same trend, increasing and then decreasing as the water-cement ratio increased. The specimens with a water-binder ratio of 0.4 and 0.7 were the first to crack, and cracks appeared after 5.5 days of energization. The crack did not appear until the test specimen with a water-binder ratio of 0.5 was energized for 6 days. Compared with ordinary concrete specimens, the steel rebar corrosion rate of foamed concrete was only 1.01% larger and the crack width was only 0.39 mm larger than that of ordinary concrete when the water-cement ratio was 0.5.

The reason for the above phenomenon is that when the water-binder ratio is relatively low, the water used to mix the slurry preparing foamed concrete is insufficient. The slurry is thicker, which affects the slurry's uniformity and causes material clumping. It is difficult to disperse the foam evenly in the slurry after it is added. The slurry is thinner when the water-binder ratio is relatively high, resulting in a slower solidification and hardening rate. At this point, the slurry is easy to separate during the pouring and maintenance process, the stability of the slurry is poor, and the excess water evaporated into the air during the mixing process will leave leakage channels for the foamed concrete. When the water-binder ratio is 0.5, the slurry can be mixed evenly, and defoaming is not easy to occur, guaranteeing the quality of foamed concrete slurry. Then it can be concluded that when the water-binder ratio is 0.5, the foamed concrete has the best corrosion resistance of steel rebar.

3.2.2 Effect of fly ash content on corrosion resistance of steel rebar

Figure 7 depicts the trends of the corrosion rate of steel rebar and the corrosion-induced cracking width with fly ash content.

It is evident that the steel rebar in the foamed concrete mixed with fly ash has stronger corrosion resistance. The corrosion rate and crack width of steel rebar showed a trend of decreasing and then increasing with the fly ash content. The corrosion rate of steel rebar and crack width are minimum at 20%, just 4.03% and 0.32 mm The cracking time of the foamed concrete specimens with different fly ash contents was dissimilar. The foamed concrete cracked earliest when the fly ash content was 40%, and the cracks appeared 6 days after energized acceleration. In comparison, the specimens with 20% and 30% content only cracked at 7 days. Compared with ordinary concrete specimens, the steel rebar corrosion rate of foamed concrete was only 0.47% larger and the crack width was only 0.23 mm larger than that of ordinary concrete when the fiber content was 20%. The above phenomenon indicates that the high fly ash content is not conducive to improving the corrosion resistance of steel rebar in foamed concrete. It can be considered that the best corrosion resistance of steel rebar is achieved when the fly ash content is 20%.

The reason for the above phenomenon is that the active components such as SiO_2 and Al_2O_3 in fly ash will react with CaO to form more stable substances, which fill the capillary pores and refine the internal structure. In addition, the smaller pore size of fly ash makes the internal structure of foamed concrete more compact, significantly reducing the porosity and the formation of through holes. However, when the content reaches 40%, the water in the foam liquid film will be absorbed and utilized by the excessive fly ash. The loss of water makes it difficult to maintain the foam form, and the phenomenon of defoaming occurs, which leads to the formation of irregular pores and the high porosity of foamed concrete. When the content of fly ash is too large, its slow-setting effect becomes more obvious, resulting in increased internal porosity of foamed concrete and decreased corrosion resistance.

3.2.3 Effect of fiber content on corrosion resistance of steel rebar

From Figure 8, it can be seen that the addition of fiber can effectively prevent the cracking of foamed concrete.

After 9 days of energized acceleration, the crack width on the foamed concrete surface was significantly reduced compared with that without fiber. The minimum corrosion rate and crack width of steel rebar were 3.75% and 0.21 mm, respectively, when the fiber dosing was 0.6%, which were 0.82% and 0.27 mm less than those without fiber. However, when the fiber content increased to 1.2%, the corrosion rate

10.3389/fmats.2022.1054662

TABLE 4 Chloride ion diffusion coefficient of foamed concrete.

Density grade	Time (d)	Surface concentration Cs (%)	Diffusion coefficient Dc (10^{-6} mm^2/s)
A04	30	0.451	37.982
	60	0.528	24.044
	90	0.594	16.822
	120	0.645	13.980
	150	0.693	12.296
A05	30	0.438	36.741
	60	0.519	23.260
	90	0.582	16.366
	120	0.635	13.173
	150	0.684	12.055
A06	30	0.426	35.056
	60	0.508	22.066
	90	0.568	15.542
	120	0.625	12.365
	150	0.674	11.461
A07	30	0.418	32.791
	60	0.499	20.631
	90	0.556	14.245
	120	0.617	11.348
	150	0.665	10.764
A08	30	0.414	28.997
	60	0.488	19.128
	90	0.543	13.106
	120	0.603	10.468
	150	0.653	9.830
A09	30	0.396	26.464
	60	0.475	16.984
	90	0.525	12.093
	120	0.592	9.679
	150	0.639	9.111
A10	30	0.371	24.614
	60	0.455	15.450
	90	0.508	11.299
	120	0.578	8.743
	150	0.618	8.575

of steel rebar and the crack width were only reduced by 0.28% and 0.09 mm compared to that without fiber. Compared with ordinary concrete specimens, the steel rebar corrosion rate of foamed concrete was only 0.19% larger and the crack width was only 0.12 mm larger than that of ordinary concrete when the fiber content was 0.60%. It can be concluded that the corrosion resistance of steel rebar of foamed concrete will worsen when the fiber content continues to increase. That is, the best corrosion resistance of steel rebar is achieved when the fiber content is 0.6%.

The main reason for the above phenomenon is that after adding the proper amount of polypropylene fiber into the foamed concrete paste, the paste and fiber penetrate each other. The fiber in the foamed concrete in a three-dimensional network structure supports the cement matrix, prevents the concrete's shrinkage, and delays the development of cracks on the concrete surface. Moreover, the fiber can also bear the corrosion expansion force generated by the corrosion products of steel rebar. And it can act together with the foam concrete's tensile stress resistance to hinder the cracks' development. However, when adding

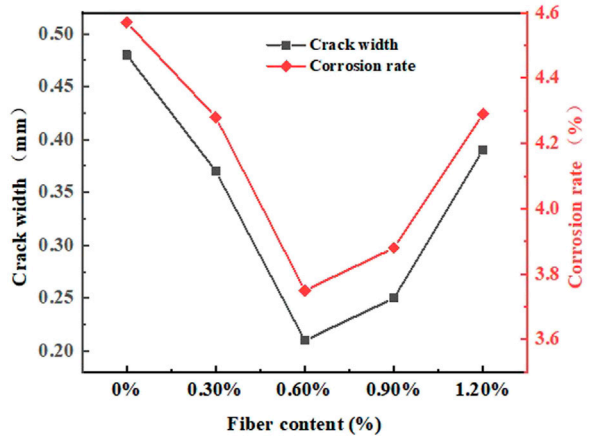

FIGURE 8
Corrosion rate and crack width with fiber content.

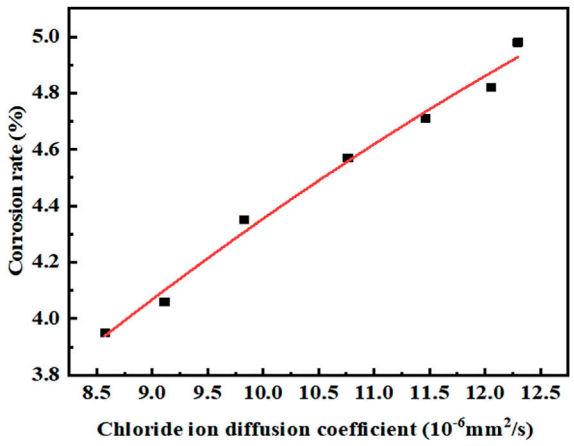

FIGURE 10
Fitted curves between chloride ion diffusion coefficient and steel rebar corrosion rate.

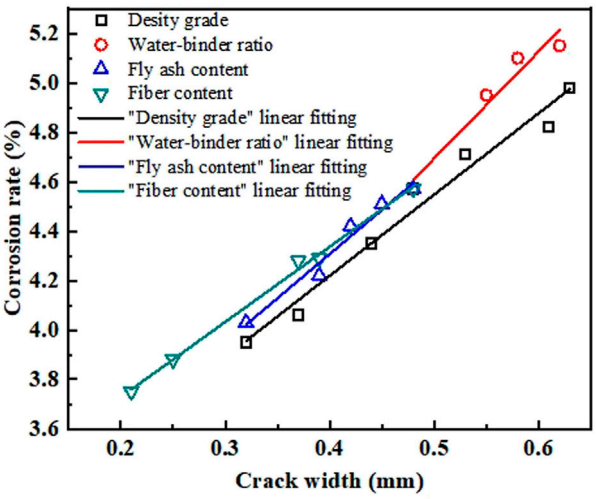

FIGURE 9
Fitted relationship between crack width and corrosion rate.

excessive fibers, some will be entangled in clumps, destroying the cement paste compatibility and resulting in increased internal defects of foamed concrete and weakened corrosion resistance.

3.3 Correlation analysis of steel rebar corrosion rate and crack width

There is a correlation between the corrosion rate of steel rebar and the crack width of foamed concrete (Vidal et al., 2004; Malumbela et al., 2010; Feng et al., 2014). Therefore, to avoid damaging the structural integrity, the corrosion behavior of steel rebar in concrete can be predicted by cracks. The relationship between the corrosion rate of steel rebar and the crack width of foamed concrete under different influencing factors is fitted based on the above experimental results, as shown in Figure 9.

From Figure 9, it can be seen that crack width and corrosion rate have a good linear correlation under each influencing factor. The correlation coefficients are 0.9687, 0.9489, 0.972 and 0.9951, respectively. Under the same corrosion condition, the greater the crack width, the crack width and the steel rebar corrosion rate are positively correlated. The corrosion of steel rebar can be predicted by observing the crack width on the foamed concrete surface. It provides a basis for determining whether the foamed concrete structure damaged by steel rebar corrosion meets the safety and durability requirements.

3.4 Determination and analysis of chloride ion diffusion coefficient

Direct measurement of chloride ion diffusion concentration in energized acceleration corrosion will accelerate ion flow, resulting in a much larger measurement than in the actual case and is not of research value. Therefore, this test obtains concrete's chloride ion diffusion concentration by natural immersion method and then calculates the chloride ion diffusion coefficient based on the concentration. When the natural immersion method is used to study the chloride ion attack on foamed concrete, chloride ions are mainly transported by diffusion. The chloride ion diffusion inside the foamed concrete follows Fick's second law (Eq. 2).

$$\frac{\partial C}{\partial t} = -D\frac{\partial^2 C}{\partial x^2} \tag{2}$$

The solution to Eq. 2 is as follows:

$$C(x,t) = C_0 + (C_s - C_0)\left[1 - erf\left(\frac{x}{2\sqrt{Dt}}\right)\right] \quad (3)$$

In Eq. 3, $C(x,t)$ is the chloride ion content at the x position of concrete at time t (%); C_0 is the initial chloride ion concentration (%) in concrete, generally taken as 0; C_s is the chloride ion concentration on the concrete surface (%); X is the diffusion depth of chloride ion (mm); D is the reference time t_0 Chloride ion diffusion coefficient at 0 (mm^2/s); $erf(x) = \frac{2}{\sqrt{\pi}}\int_0^x e^{-z^2}dz$ is a Gaussian error function.

The measurement results are shown in Table 4. It can be seen that the higher the density grade of the foamed concrete, the better the chloride ion diffusion coefficient. That is, the higher the grade, the more resistant the foamed concrete is to chloride ion penetration. This phenomenon is consistent with the corrosion behavior of steel rebar in foamed concrete of different density grades, so the chloride ion penetration resistance of foamed concrete can reflect the corrosion resistance of steel rebar to some extent.

After 150 days of natural immersion, the chloride ion diffusion coefficient has gradually remained stable. Therefore, the chloride diffusion coefficients of foamed concrete of each density class immersed for 150 days can be used for correlation analysis. The fitted curves of chloride ion diffusion coefficient and steel rebar corrosion rate are shown in Figure 10. It can be seen that there is an apparent quadratic function relationship between chloride ion diffusion coefficient and steel rebar corrosion rate. The fitting equation is $y = -0.0113x^2 + 0.501x + 0.472$, fitted correlation $R^2 = 0.9836$. It can be concluded that the foamed concrete with better resistance to chloride ion penetration has the same good rust resistance in a specific range of foamed concrete density grades.

4 Conclusion

The following conclusions can be drawn from the results of this study.

(1) With time increased, the steel rebar corrosion rate of foamed concrete and the crack width shows a trend of first slowly increasing, then rapidly developing, and finally slowly increasing. Furthermore, the greater the density grade of foamed concrete, the smaller the steel rebar corrosion rate, and the maximum crack width on the specimen's surface gradually decreases. That is, the stronger the corrosion resistance of steel rebar. It is found that the density grade of foamed concrete has an exponential function relationship with the steel rebar corrosion rate and the crack width.

(2) It can be seen that with the water-binder ratio increased, the steel rebar corrosion rate decreases first and then increases. At the same time, the admixture of fly ash and fiber can significantly improve the corrosion resistance of steel rebar in foamed concrete specimens. However, when the amount of fly ash and fiber is too large, it will decrease the corrosion resistance of steel rebar. It can be concluded that when the water-binder ratio is 0.5, and the fly ash and fiber dosing are 20% and 0.6%, respectively, the corrosion resistance of steel rebar of foamed concrete is the best.

(3) The linear curve fit values of crack width and steel rebar corrosion rate under each influencing factor were obtained. Experimental support was provided for the correlation between the steel rebar corrosion rate and the crack width of foamed concrete.

(4) The higher the density grade, the better the chloride ion diffusion coefficient of the foamed concrete. That is, the stronger the resistance to chloride ion penetration. In a specific density grade range, foamed concrete's chloride ion diffusion coefficient positively correlates with the steel rebar corrosion rate (Figures 9, 10).

Data availability statement

The original contributions presented in the study are included in the article/supplementary material, further inquiries can be directed to the corresponding authors.

Author contributions

QZ, YL, SP conducted all of the experimental studies and analyzed the test data. DC and CL advised the theoretical research and experimental work and revised the manuscript. All authors have read and agreed to the published version of the manuscript.

Funding

This research was supported by the National Key Research and Development Program of China (No. 2021YFB3802005), and the National Natural Science Foundation of China (Grant No. 51978002).

Acknowledgments

The authors gratefully acknowledge the National Natural Science Foundation and the National Key Research and Development Program of China for financial. The authors would like to express our gratitude to Anhui University of Technology for providing various research conditions to facilitate this work.

Conflict of interest

Author QZ is employed by Shanghai Jianke Engineering Consulting Co., Ltd.

The remaining authors declare that the research was conducted in the absence of any commercial or financial relationships that could be construed as a potential conflict of interest.

Publisher's note

References

Ahmad, S. (2003). Reinforcement corrosion in concrete structures, its monitoring and service life prediction–a review. *Cem. Concr. Compos.* 25 (4-5), 459–471. doi:10.1016/s0958-9465(02)00086-0

Al-Harthy, A. S., Stewart, M. G., and Mullard, J. (2011). Concrete cover cracking caused by steel reinforcement corrosion. *Mag. Concr. Res.* 63 (9), 655–667. doi:10.1680/macr.2011.63.9.655

Amran, Y., Farzadnia, N., and Ali, A. (2015). Properties and applications of foamed concrete; a review. *Constr. Build. Mat.* 101, 990–1005. doi:10.1016/j.conbuildmat.2015.10.112

Falliano, D., Domenico, D. D., Ricciardi, G., and Gugliandolo, E. (2019). Compressive and flexural strength of fiber-reinforced foamed concrete: Effect of fiber content, curing conditions and dry density. *Constr. Build. Mat.* 198, 479–493. doi:10.1016/j.conbuildmat.2018.11.197

Feng, W. U., Gong, J. H., and Zhang, Z. (2014). Calculation of corrosion rate for reinforced concrete beams based on corrosive crack width. *J. Zheijang. Univ. -Sci.* 15 (3), 197–207. doi:10.1631/jzus.a1300280

Ganiron, T. U. (2016). Development and efficiency of prefabricated building components. *Int. J. Smart Home* 10 (6), 85–94. doi:10.14257/ijsh.2016.10.6.10

Gu, X. (2018). Analysis of the restrictive factors and countermeasures for the development of prefabricated buildings. *Jiangxi Build. Mater.* 13, 3–4.

Ha, T. H., Muralidharan, S., Bae, J. H., Ha, Y. C., Lee, H. G., Park, K. W., et al. (2007). Accelerated short-term techniques to evaluate the corrosion performance of steel in fly ash blended concrete. *Build. Environ.* 42 (1), 78–85. doi:10.1016/j.buildenv.2005.08.019

Hilal, A. A., Thom, N. H., and Dawson, A. R. (2015). On entrained pore size distribution of foamed concrete. *Constr. Build. Mater.* 75, 227–233. doi:10.1016/j.conbuildmat.2014.09.117

Huet, B., L'Hostis, V., Miserque, F., and Idrissi, H. (2006). Electrochemical behavior of mild steel in concrete: Influence of pH and carbonate content of concrete pore solution. *Electrochimica Acta* 51 (1), 172–180. doi:10.1016/j.electacta.2005.04.014

Jones, M. R., and Mccarthy, A. (2005). Utilising unprocessed low-lime coal fly ash in foamed concrete. *Fuel* 84 (11), 1398–1409. doi:10.1016/j.fuel.2004.09.030

Lee, Y. L., Zaidi, A. A., Koh, H. B., Sulaiman, S., Adnan, S. H., and Rahman, I. (2011). Carbonation and water permeability of foamed concrete. *Int. J. Sustain. Constr. Eng. Technol.* 1 (1), 261–270.

Li, C. Q., and Melchers, R. E. (2005). Time-dependent reliability analysis of corrosion-induced concrete cracking. *Aci Struct. J.* 102 (4), 543–549.

Liu, P. C., Wu, X., Chen, H. Y., Li, T. J., and Hu, Y. (2020). "Multi objective optimization of mix proportion of foam concrete[C]," in Conference Proceedings of the 8th International Symposium on Project Management, China (ISPM2020), 518–524.

Maaddawy, T. E., and Soudki, K. (2007). A model for prediction of time from corrosion initiation to corrosion cracking. *Cem. Concr. Compos.* 29 (3), 168–175. doi:10.1016/j.cemconcomp.2006.11.004

Maaddawy, T., and Soudki, K. A. (2003). Effectiveness of impressed current technique to simulate corrosion of steel reinforcement in concrete. *J. Mat. Civ. Eng.* 15 (1), 41–47. doi:10.1061/(asce)0899-1561(2003)15:1(41)

Malumbela, G., Alexander, M., and Moyo, P. (2010). Lateral deformation of RC beams under simultaneous load and steel corrosion. *Constr. Build. Mat.* 24 (1), 17–24. doi:10.1016/j.conbuildmat.2009.08.005

Marsavina, L., Audenaert, K., Schutter, G. D., Faur, N., and Marsavina, D. (2007). Experimental and numerical determination of the chloride penetration in cracked concrete. *Constr. Build. Mater.* 23 (1), 599–607. doi:10.1016/j.conbuildmat.2007.12.015

Namsone, E., Šahmenko, G., and Korjakins, A. (2017). Durability properties of high performance foamed concrete. *Procedia Eng.* 172, 760–767. doi:10.1016/j.proeng.2017.02.120

Remennikov, A. M., Kong, S. Y., and Uy, B. (2011). Response of foam- and concrete-filled square steel tubes under low-velocity impact loading. *J. Perform. Constr. Facil.* 25 (5), 373–381. doi:10.1061/(asce)cf.1943-5509.0000175

Roslan, A. F., Awang, H., and Mydin, M. A. O. (2012). Effects of various additives on drying shrinkage, compressive and flexural strength of lightweight foamed concrete (LFC). *Adv. Mat. Res.* 626, 594–604. doi:10.4028/www.scientific.net/amr.626.594

Sabine, C., and Raharinaivo, A. (2007). Influence of impressed current on the initiation of damage in reinforced mortar due to corrosion of embedded steel. *Cem. Concr. Res.* 37 (12), 287–296. doi:10.1016/j.cemconres.2007.08.022

Shi, J., and Xu, Y. (2007). Estimation and forecasting of concrete debris amount in China. *Resour. Conserv. Recycl.* 49 (2), 147–158. doi:10.1016/j.resconrec.2006.03.011

Surendranath, Y., and Harman, W. D. (2006). The role of electrochemistry in the development of pi-basic dearomatization agents. *Dalton Trans.* 33, 3957–3965. doi:10.1039/b607694g

Tang, F., Lin, Z., Chen, G., and Yi, W. (2014). Three-dimensional corrosion pit measurement and statistical mechanical degradation analysis of deformed steel bars subjected to accelerated corrosion. *Constr. Build. Mat.* 70, 104–117. doi:10.1016/j.conbuildmat.2014.08.001

Vidal, T., Castel, A., and François, R. (2004). Analyzing crack width to predict corrosion in reinforced concrete. *Cem. Concr. Res.* 34 (1), 165–174. doi:10.1016/s0008-8846(03)00246-1

Vu, K., and Stewart, M. G. (2005). Predicting the likelihood and extent of reinforced concrete corrosion-induced cracking. *J. Struct. Eng. (N. Y. N. Y).* 131 (11), 1681–1689. doi:10.1061/(asce)0733-9445(2005)131:11(1681)

Xiong, L., and Shen, J. (2019). Analysis of the development and trend of China's prefabricated buildings. *IOP Conf. Ser. Earth Environ. Sci.* 371 (2), 022043–43. doi:10.1088/1755-1315/371/2/022043

Zhang, J., Jiang, N., Hui, L., and Wu, C. (2018). Study on mix proportion design of cement foam concrete. *IOP Conf. Ser. Mat. Sci. Eng.* 439 (4), 042053–53. doi:10.1088/1757-899x/439/4/042053